Biophysical *Journal*
Article

Biophysical Society

The Long-Chain Sphingoid Base of Ceramides Determines Their Propensity for Lateral Segregation

Md. Abdullah Al Sazzad,[1] Tomokazu Yasuda,[1,2] Michio Murata,[2] and J. Peter Slotte[1,*]
[1]Biochemistry, Faculty of Science and Engineering, Åbo Akademi University, Turku, Finland; and [2]Department of Organic Chemistry, Graduate School of Science, University of Osaka, Osaka, Japan

ABSTRACT We examined how the length of the long-chain base or the *N*-linked acyl chain of ceramides affected their lateral segregation in 1-palmitoyl-2-oleoyl-*sn*-glycero-3-phosphocholine (POPC) bilayers. Lateral segregation and ceramide-rich phase formation was ascertained by a lifetime analysis of *trans*-parinaric acid (tPA) fluorescence. The longer the length of the long-chain base (d16:1, d17:1, d18:1, d19:1, and d20:1 in *N*-palmitoyl ceramide), the less ceramide was needed for the onset of lateral segregation and ceramide-rich phase formation. A similar but much weaker trend was observed when sphingosine (d18:1)-based ceramide had *N*-linked acyl chains of increasing length (14:0 and 16:0–20:0 in one-carbon increments). The apparent lateral packing of the ceramide-rich phase, as determined from the longest-lifetime component of tPA fluorescence, also correlated strongly with the long-chain base length, but not as strongly with the *N*-acyl chain length. Finally, we compared two ceramide analogs with equal carbon numbers (d16:1/17:0 or d20:1/13:0) and observed that the analog with a longer sphingoid base segregated at lower bilayer concentrations to a ceramide-rich phase compared with the shorter sphingoid base analog. The gel phase formed by d20:1/13:0 ceramide also was more thermostable than the gel phase formed by d16:1/17:0 ceramide. ^{2}H NMR data for 10 mol % stearoyl ceramide in POPC also showed that the long-chain base was more ordered than the acyl chain at comparable chain positions and temperatures. We conclude that the long-chain base length of ceramide is more important than the acyl chain length in determining the lateral segregation of the ceramide-rich gel phase and intermolecular interactions therein.

INTRODUCTION

Ceramides are the direct building blocks of complex sphingolipids such as sphingomyelins (SMs), cerebrosides, gangliosides, and sulfatides (1–3). Besides their precursor role in sphingolipid biosynthesis, ceramides are important constituents in the skin, where they contribute to its permeability barrier function (4,5). Ceramides are also implicated as effectors of various cellular activities and signaling cascades (6). The ceramide molecule consists of a sphingoid long-chain base (often 2-amino-4-octadecene-1,3-diol, or sphingosine (d18:1)) to which saturated acyl chains are often *N*-linked (7). However, the length and nature of the sphingoid long-chain base vary among various tissues and organisms (8), as does the length of the *N*-linked acyl chain. Both the nature and the length of the sphingoid base and the acyl chains are generally known to affect the biophysical properties of ceramides (and sphingolipids) in bilayer membranes (9–15).

It has been shown that the gel-phase melting temperature (T_m) of ceramides (in complexes with saturated SM) increases with increasing long-chain base lengths (11), but not as clearly with increasing *N*-linked acyl chain lengths (12). In 1-palmitoyl-2-oleoyl-*sn*-glycero-3-phosphocholine (POPC) bilayers, 20 mol % saturated stearoyl ceramide showed lower thermostability than saturated palmitoyl ceramide, but the difference disappeared at higher ceramide concentrations (16). For the long-chain base analogs, the results can be understood to relate to increased van der Waals attractive forces among the ceramides. However, for some reason, the acyl chain length does not appear to affect interactions in the ceramide-rich ordered phase to a similar extent as the long-chain base. Increased unsaturations of both the long-chain base and the acyl chains (12) appear to have stronger effects on ceramide-rich phase stability and intermolecular interactions. Hydrogen bonding involving the functional groups of the sphingoid base also affects intermolecular interactions (17). It is known that in biological systems, long saturated acyl chains are important for the function of ceramides in the skin, as shortening of the ceramide acyl chains leads to increased water permeabilization of the skin (18).

Submitted November 4, 2016, and accepted for publication January 24, 2017.

*Correspondence: jpslotte@abo.fi

Editor: Heiko Heerklotz.
http://dx.doi.org/10.1016/j.bpj.2017.01.016

In bilayers mimicking cellular plasma membranes, ceramide has been shown to displace cholesterol and prevent it from interacting with saturated phospholipids such as dipalmitoyl phosphatidylcholine (19) and palmitoyl SM (PSM) (20). The cholesterol-displacing effect is dependent on the ceramide acyl chain length (12,13) and on the balance of cholesterol and ceramide in the bilayer (21,22). The propensity for lateral segregation of ceramides in fluid phosphatidylcholine bilayers is affected by the length of the long-chain base, by the nature of the *N*-linked acyl chain, and by the hydrogen-bonding properties of the ceramides (23). However, it is not fully understood how ceramide interactions in bilayers are affected by the asymmetric nature of the molecule.

Ceramide asymmetry rises from the two unequal long chains in the molecule (the long-chain base and the *N*-linked acyl chain) and from hydrogen-bonding functional groups found on the long-chain base. In addition, ceramides may show a chain-length mismatch if the long-chain base is much longer or shorter than the *N*-linked acyl chain. Also, we do not know whether ceramide shows any asymmetric interaction with membrane lipids. As an example, it can be assumed that a saturated ceramide-POPC interaction is likely to involve the palmitoyl chain of POPC (24), but is the palmitoyl residue interacting more with the long-chain base or with the *N*-linked acyl chain of the ceramide? A recent molecular-dynamics simulation study of ceramide in 1,2-dimyristoyl-phosphatidylcholine (DMPC) bilayers suggested that both the long-chain base and the *N*-linked acyl chain are equally ordered in the presence of DMPC, which may suggest no asymmetric interaction (25).

To date, no systematic comparative studies of the effects of long-chain base length and acyl chain length on ceramide behavior in unsaturated phospholipid bilayers have been performed. In this study, we used chemical synthesis to prepare a range of saturated ceramides with variable long-chain base and acyl chain lengths. We systematically examined their lateral segregation in POPC bilayers via a lifetime analysis of *trans*-parinaric acid (tPA) fluorescence, since the lifetime of tPA is very sensitive both to the formation of an ordered phase and to the lateral packing in the ordered phase (26). We observed that the length of the long-chain base was much more important for determining lateral segregation in POPC bilayers than the length of the *N*-linked acyl chain. This may suggest that ceramides interact asymmetrically with colipids and that interactions involving the long-chain base are preferred for ceramide-rich phase stabilization.

MATERIALS AND METHODS

Materials

POPC, palmitoyl ceramide (PCer or d18:1/16:0 ceramide), and sphingoid D-*erythro*-long-chain bases (with lengths of 14, 16–18, and 20 carbons) were obtained from Avanti Polar Lipids (Alabaster, AL) or Larodan (Stockholm, Sweden). Saturated fatty acids (14:0 and 16:0–20:0) were obtained from Larodan. The methyl ester of α-linolenic acid was obtained from Sigma-Aldrich (St. Louis, MO).

Ceramides with the indicated sphingoid bases and acyl chains were synthesized by coupling the fatty anhydride to the long-chain base in the presence of triethylamine as described previously (27). For the structures of the molecules, see Scheme S1 in the Supporting Material. The fatty anhydride was prepared with *N*,*N*-dicyclohexylcarbodiimide. The d19:1 long-chain base is not commercially available, and the d19:1/16:0 ceramide was synthesized as described in the Supporting Material. tPA was prepared from the methyl ester of α-linolenic acid as described previously (28) and purified by crystallization from hexane (26). tPA ceramide (tPA-Cer) was prepared from tPA and sphingosine. The identities of the long-chain bases, the fatty acids used for synthesis, and the products obtained (various ceramides) were verified by electrospray ionization mass spectrometry (Bruker Daltonics, Billerica, MA) or NMR (d19:1/16:0 ceramide).

Vesicle preparation

Multilamellar lipid vesicles (MLVs) for lifetime measurements were prepared from the indicated lipids to a final total lipid concentration of 0.2 mM. The lipids were mixed in an organic solvent before the solvent was evaporated at 40°C under a stream of nitrogen gas. The dry lipids were kept in a vacuum for 3 h before hydration. The lipids were hydrated in pure water at 70°C for 1 h, followed by vortex mixing (2–3 min) and bath sonication at 70°C (5 min). Immediately after hydration, tPA was added (1 mol %) to the hot MLVs from an ethanolic stock solution. The final ethanol concentration was 0.2 vol %. The vesicles were cooled to room temperature before use. The tPA-containing vesicles were not exposed to white light during processing.

Lifetime analysis of tPA

MLVs were prepared as described above. Time-resolved fluorescence experiments were performed using a FluoTime 200 spectrofluorimeter with a PicoHarp 300E time-correlated single photon counting module (PicoQuant, Berlin, Germany). A 297-nm LED laser source (PLS300; PicoQuant) was used for excitation of tPA, and an emission was detected at 405 nm. The fluorescent decays were analyzed using the software FluoFit Pro (PicoQuant). The decays were very similar for both 1 mol % tPA and 0.2 mol % tPA, indicating that the probe concentration did not measurably affect the fluorescence lifetime (results not shown). The data were fitted to contain two or three lifetime components (whichever gave the best unbiased residual plots) and χ-squared closest to one. The average lifetime was calculated as described in Lakowicz (29).

tPA-Cer anisotropy measurements

Steady-state anisotropy of tPA-Cer in MLVs was measured with a QuantaMaster 1 instrument (Photon Technology International, Edison, NJ). tPA-Cer was used instead of tPA as the end-of-gel-phase T_m was clearer with tPA-Cer than with tPA for some of the ceramide analogs. The overall anisotropy function was very similar with both tPA probes. The excitation polarizer was in the vertical position (0°) and the emission polarizers were switched between the vertical (0°) and horizontal (90°) positions for each measurement point. The G-factor (the ratio of sensitivities of the detection system for vertically and horizontally polarized light) was determined with the excitation polarizer in the horizontal position (90°). The anisotropy was calculated according to (29):

$$r = (I_{VV} - GI_{VH})/(I_{VV} + 2GI_{HV}),$$

where I is the intensity measured with a vertical (V) or horizontal (H) polarizer plane (the first letter is for the excitation polarizer, the second for the

emission polarizer). The anisotropy of samples containing the indicated lipids and 1 mol % tPA-Cer (mixed together with other lipids before hydration) was recorded between 5°C and 60°C using a temperature ramp of 2°C/min. The excitation and emission wavelengths were 305 and 405 nm, respectively, for tPA.

Sample preparation and measurements of ^{2}H NMR

Sample preparation and ^{2}H NMR measurements were conducted in a manner similar to that described in our previous work (30). The bilayers were composed of POPC with 10 mol % stearoyl ceramide, which had site-specific deuteration at 12,12 in the long-chain base or at 10′,10′ of the stearoyl chain. The lipid mixtures were dissolved in MeOH-$CHCl_3$ and the solvents were evaporated, after which they were kept in vacuo overnight. MLVs were prepared by hydrating the dried lipid films with ~1 mL of deuterium-depleted water at 65°C, followed by vigorous vortexing. Each suspension was freeze-thawed 10 times, followed by lyophilization, rehydration with deuterium-depleted water until 50% hydration was achieved (w/w), and freeze-thawed 10 times again. Each sample was transferred into a 5 mm glass tube (Wilmad, Vineland, NJ) that was sealed with epoxy glue. All of the ^{2}H NMR spectra were recorded on a 300 MHz CMX300 spectrometer (Chemagnetics, Agilent, Palo Alto, CA) fitted with a 5 mm ^{2}H static probe (Otsuka Electronics, Osaka, Japan) using a quadrupolar echo sequence. The 90° pulse width was 2.5 μs, the interpulse delay was 30 μs, and the repetition rate was 0.6 s. The sweep width was 250 kHz and the number of scans was ~100,000.

RESULTS

Lateral segregation of ceramide analogs in POPC bilayers

To examine how the chain length of the long-chain bases affected lateral segregation and ceramide-rich phase formation in pure POPC bilayers, we prepared the POPC bilayers to contain increasing amounts of ceramide analogs with different long-chain bases but the same *N*-linked palmitoyl chain. We measured the tPA fluorescence lifetime at 23°C. The lifetime of tPA increased markedly as soon as it partitioned from a disordered into an ordered or ceramide-rich phase (23,31). Its partition coefficient toward ordered phases was high compared with the situation in disordered phases (32). The concentration of d18:1/16:0 ceramide needed for gel-phase onset, as reported by an increased tPA lifetime (see Fig. 1 here and Fig. 1 in (23)), agreed well with differential scanning calorimetry data for similar bilayer compositions (Fig. S1), validating the use of tPA lifetime analysis to register the formation of ceramide-enriched ordered domains in bilayer membranes.

As shown in Fig. 1 *A*, the intensity-weighted average lifetime of tPA increased with increasing bilayer ceramide content. The ceramide analogs with the longest long-chain base formed a ceramide-rich phase at the lowest bilayer concentration (the ceramide-rich phase formed above 2.5 mol % for 20:1-PCer), and as the long-chain base became shorter, more and more ceramide analog was needed to form a ceramide-rich phase at 23°C. 14:1-PCer failed to form a ceramide-rich phase at the highest concentration tested (30 mol %; data not shown). The lifetime of tPA fluorescence usually contains three lifetime components, and the longest of these is believed to report from the most ordered phase present (here, the ceramide-rich phase). In Fig. 1 *B*, the longest-lifetime component of tPA fluorescence is plotted against the ceramide content in the POPC bilayers. The concentrations needed to form a ceramide-rich phase by the different long-chain base analogs were reported similarly by the longest-lifetime component as given by the average lifetime (Fig. 1 *A*).

For the analogs having long-chain base lengths of 16 and 20 carbons, the longest-lifetime component reached a plateau in the concentration range examined. The length of the longest-lifetime components at the plateau differed for the different analogs (Fig. 1 *B*). The longest component

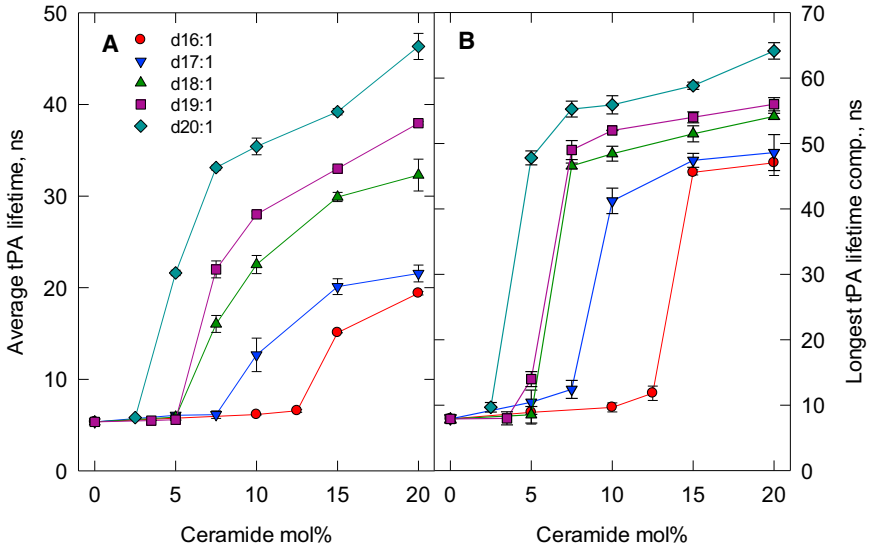

FIGURE 1 Lateral segregation of palmitoyl ceramide analogs with different long-chain base lengths in POPC bilayers at 23°C. (*A*) Intensity-weighted average lifetime of tPA fluorescence in bilayers as a function of ceramide concentration. (*B*) Intensity-based longest-lifetime component of tPA fluorescence as a function of ceramide concentration. All ceramide analogs had an *N*-linked palmitoyl acyl chain. Each value is the average ± SEM; n = 2–3; ns, nanoseconds. To see this figure in color, go online.

lifetime was ~60–64 ns for 20:1-PCer, and with a shortening long-chain base, the lifetime decreased with chain length to ~47 ns for 16:1-PCer.

Next, we examined how varying the length of the *N*-linked acyl chain in d18:1-based ceramides affected their lateral segregation in POPC bilayers at 23°C. As shown in Fig. 2 *A*, the *N*-linked acyl chain length had very small effects on the concentration of ceramide needed to form a ceramide-rich phase in the POPC bilayer. From the plot of the longest-lifetime component of tPA fluorescence (Fig. 2 *B*), it can be noted that the ceramide-rich phase that formed appeared to have very similar packing properties, as the longest component lifetime was similar for all acyl chain analogs with lengths of C16 or longer (C-14:0 showed a slightly shorter lifetime of the longest-lifetime component compared with the longer acyl chain analogs).

Ceramide gel-phase stability as a function of the long-chain base and acyl chain length

We also determined the thermostability of the ceramide-rich phase in POPC bilayers at a 1:9 molar ratio as a function of temperature. Ceramide-rich-phase melting was determined from an anisotropy analysis of tPA-Cer fluorescence as described previously (24). The end temperature of ceramide-rich-phase melting for ceramide/POPC bilayers gives an almost identical result when measured from tPA anisotropy or differential scanning calorimetry (24). Fig. 3 shows the end temperature of ceramide-rich-phase melting for the long-chain base or acyl chain length analogs of the ceramides in POPC bilayers (the original anisotropy curves are shown in Figs. S2 and S3). It was observed that the length of the long-chain base in palmitoyl ceramide had a much larger effect on ceramide-rich phase stability compared with d18:1-based ceramides with *N*-linked acyl chains varying from 14:0 to 20:0 (Fig. 3). These results agree with the results from Fig. 1 and show much larger effects of the long-chain base length on lateral segregation and ceramide-rich phase formation when compared with the acyl chain analogs of ceramides. The main T_m values of pure hydrated ceramides in water are shown in Table S1. The T_m of the ceramides varied more when the long-chain base length was varied (T_m = 82.4–96.4°C going from d15:1 to d20:1 base length), and less when the acyl chain length was different (T_m = 91.5°C for the 16:0 acyl chain analog and 92.6°C for the 20:0 acyl chain analog). This finding is consistent with the suggestion that the long-chain base length is also more dominant for intermolecular interactions among ceramides.

Behavior of asymmetric ceramide analogs in POPC bilayers

To more carefully compare the effects of the long-chain base and the *N*-linked acyl chain on lateral segregation and ceramide-rich phase stability, we prepared two asymmetric ceramide analogs (Fig. 4 *A*). Both analogs had an equal number of carbons in the chains (sum of carbons in long-chain base and acyl chain = 33), but the length of these chains was varied to create the asymmetry. We observed that the analog with the longer long-chain base (d20:1/13:0) segregated to a ceramide-rich phase at a lower bilayer concentration (>7 mol %) compared with the ceramide analog with a shorter long-chain base (d16:1/17:0) (~12.5 mol %; Fig. 4 *B*). When the thermostability of the POPC/Cer analog gel phase was determined (using tPA anisotropy to reveal the end temperature of gel-phase melting), it was observed that the ceramide analog with the longer long-chain base was slightly more thermostable than the shorter long-chain base analog (Fig. 4 *C*). These results suggest that

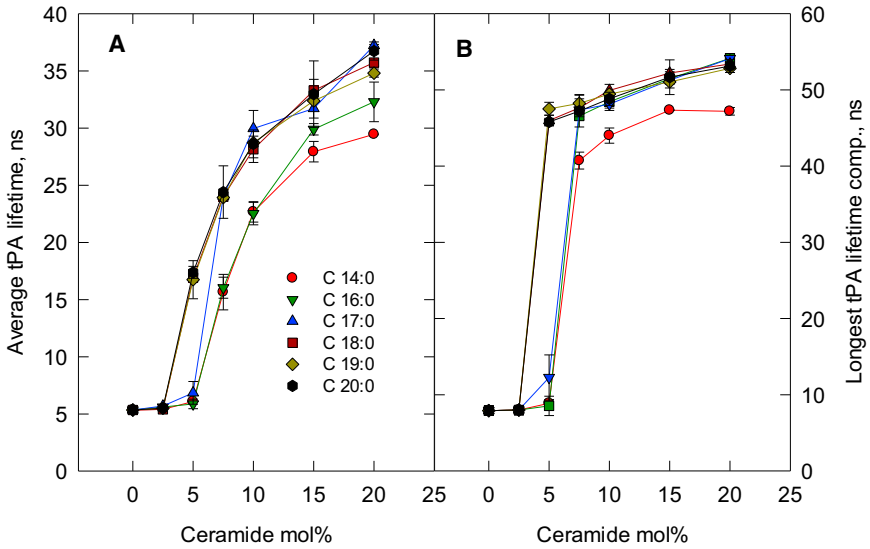

FIGURE 2 Lateral segregation of sphingosine (d18:1)-based ceramide analogs with saturated acyl chains of different lengths in POPC bilayers at 23°C. (*A*) Intensity-weighted average lifetime of tPA fluorescence in bilayers as a function of ceramide concentration. (*B*) Intensity-based longest-lifetime component of tPA fluorescence as a function of ceramide concentration. All ceramide analogs had sphingosine (d18:1) as a long-chain base. Each value is the average ± SEM; n = 2–3; ns, nanoseconds. To see this figure in color, go online.

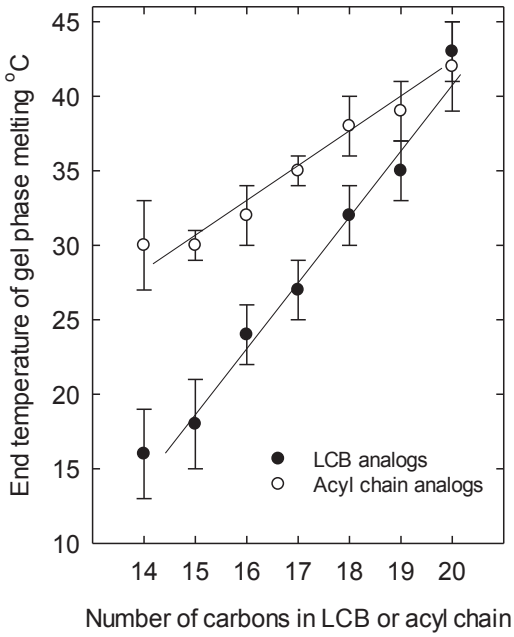

FIGURE 3 End melting temperature of the ceramide/POPC phase as a function of long-chain base length or acyl chain length. The POPC bilayers contained 10 mol % ceramide analog, and the end T_m of the ceramide-rich phase was determined from tPA-Cer anisotropy measurements. Each value is the average ± SEM; $n = 2–3$; LCB, long-chain base.

the long-chain base length had a greater effect on ceramide-rich gel phase formation and thermostability than the acyl chain length.

To further verify this observation, we measured the long-chain base or acyl chain order in site-deuterated d18:1/18:0 ceramides and compared the quadrupolar splitting value ($\Delta\nu$) of 12,12-d2-labeled long-chain base and 10′,10′-d2-labeled stearoyl chain as a function of temperature. The 12 position on the long-chain base has been reported to reside at the same depth as the 10′ position on a stearoyl chain in the bilayer of SM (30). As can be seen in Fig. 5, the $\Delta\nu$ values were significantly higher for the 12,12-d2 carbon of the long-chain base than for the 10′,10′-d2-carbon of the stearoyl moiety in the temperature range of 20–30°C; however, with increasing temperatures the difference disappeared. ^{2}H NMR spectra are shown in Figs. S4 and S5. The fluorescence experiments (e.g., Fig. 3) revealed that d18:1/18:0 Cer (10 mol %) in POPC underwent phase segregation at 23°C and the ordered domain melted at 33°C. In contrast, the ^{2}H NMR spectra of both d18:1-12,12-d_2-ceramide and 18:0-10′,10′-d_2-ceramide in POPC showed mixed signals of a broad component and sharp Pake doublet at 20°C and 25°C, and the broad signal almost disappeared at 30°C. Since the gel phase usually gives rise to a broad peak, these spectra indicate that the gel and liquid-disordered phases segregate at low temperature, which is in parallel with the melting of the gel phase observed in the fluorescence experiments (Fig. 3). Further, the mobility (^{2}H Pake splitting) of the two chains of ceramide became similar at 35°C since the mobility of all the alkane chains should be equal in a single-phase membrane. Interestingly, a similar difference in the order of the long-chain base (C12) and the stearoyl moiety (C10) was not seen for SM in POPC (Fig. S6).

DISCUSSION

In fluid phospholipid bilayers, saturated ceramides are known to laterally segregate into ceramide-rich gel phases (23,31,33–37). This segregation is, in part, due to ceramide lacking a large headgroup to protect its hydrophobic parts from unfavorable exposure to interfacial water (38–40). Saturated ceramide may also laterally segregate to avoid

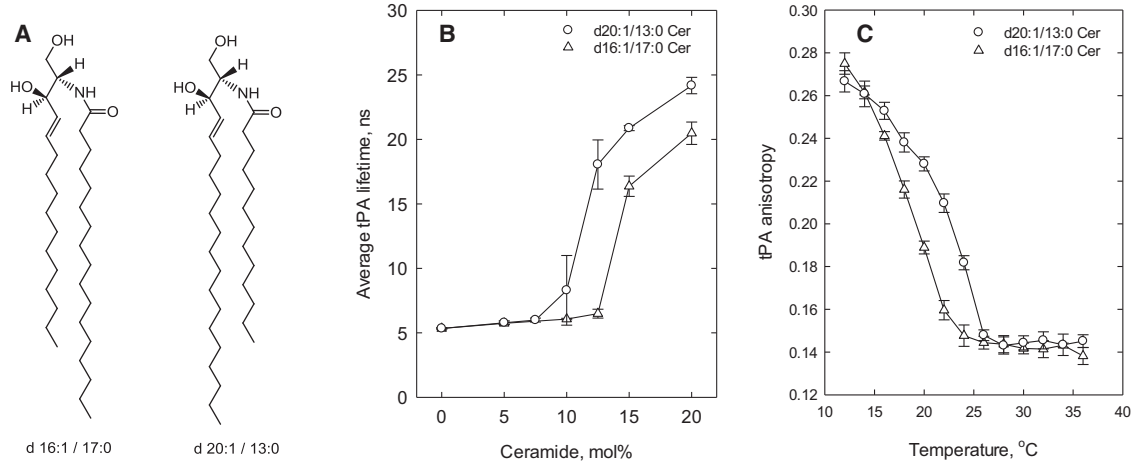

FIGURE 4 Effect of asymmetric analogs of ceramide on lateral segregation and gel-phase thermostability in POPC bilayers, as determined by tPA fluorescence lifetime analysis and anisotropy. The ceramide analogs had either a long-chain base of d16:1 or d20:1, or an *N*-linked acyl chain of 17:0 or 13:0. (*A*) Chemical structure of the two ceramide analogs. (*B*) Intensity-weighted average lifetime of tPA fluorescence. (*C*) Thermostability of the ceramide-rich gel phase based on tPA anisotropy measurements. The composition in (*C*) was 10 mol % ceramide analog in POPC. Each value is the average ± SEM; $n = 3$; ns, nanoseconds.

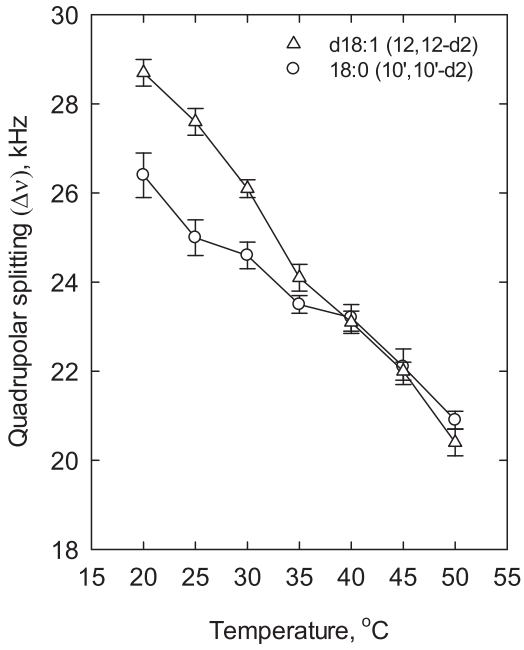

FIGURE 5 Order profile of a site-deuterated long-chain base or acyl chain in stearoyl ceramide. In the ceramide, either the sphingosine long-chain base was site deuterated (d2) at carbon 12 or the stearoyl acyl chain was site deuterated at carbon 10. The quadrupolar splitting ($\Delta\nu$) was determined as a function of temperature for the two ceramide analogs. The ceramide content was 10 mol % in POPC. Each value is the average ± SEM; $n = 2$.

interactions with disordered acyl chains and favor interactions with saturated acyl chains (24). Hydrogen bonding involving the 2NH is known to be important for the stabilization of ceramide gel phases (17,23), and the 1-OH is also likely to be involved in interfacial hydrogen bonding. Methylation of the 3-OH does not appear to interfere with the lateral segregation of the ceramide analog; thus, hydrogen bonding involving the 3-OH may not be very critical (23).

We systematically examined the lateral-segregation tendency of ceramide analogs in which either the long-chain base length or the *N*-linked acyl chain length varied. Lateral segregation was ascertained from changes in the fluorescence lifetime of tPA, which is a probe with high affinity for the ceramide-rich phase. The effects of a long-chain base length on ceramide-SM interactions were previously examined and it was found that the long-chain base length influenced the thermostability of equimolar ceramide/SM mixed bilayers (11). Interestingly, the acyl chain length did not seem to affect the thermostability of equimolar ceramide/SM mixed bilayers (12). However, the effects of long-chain base or acyl chain lengths on the lateral segregation of ceramides in fluid phosphatidylcholine bilayers have not been examined under carefully controlled conditions.

We observed that variations of the long-chain base length had a more dramatic effect both on the concentration needed for the ceramide to segregate laterally into a gel phase in POPC bilayers (Fig. 1) and on the thermostability of the gel phase (Fig. 3) compared with variations of the acyl chain length (Fig. 2). In binary mixed bilayers containing PSM and ceramide analogs with long-chain bases of different lengths, the gel-phase T_m also shifted to a higher temperature as the long-chain base length increased (11), showing a behavior in PSM bilayers similar to that observed in our POPC bilayer system. However, in equimolar-mixed bilayers of PSM and acyl chain length ceramide analogs (C16:0, C18:0, and C24:0), the T_m of the main gel-phase transition was centered at 72–74°C, irrespective of the acyl chain length (12), whereas the gel-phase stability was moderately affected in pure POPC bilayers by varying acyl chain lengths (Fig. 3). The gel-phase-onset concentration of ceramides (Fig. 1) should correlate with the T_m of the pure ceramide, since both the T_m and ΔH affect miscibility in binary bilayers (41). We see that it does, since the long-chain base ceramides displayed significantly different T_m values as a function of chain length when compared with the acyl chain analogs of ceramides (Table S1). Unfortunately, we do not have reliable gel-phase melting enthalpies to correlate our results with phase rule predictions.

Our findings with ceramide analogs in POPC bilayers suggest that ceramide interactions with POPC are asymmetric, for two reasons: 1) since POPC is a hybrid lipid (42), a saturated colipid is more likely to interact with the palmitoyl residue than with the oleoyl residue of POPC; and 2) the ceramides apparently interacted with the palmitoyl residue of POPC mainly via the long-chain base and not so much via the saturated *N*-linked acyl chain, because the long-chain base affected intermolecular interactions more strongly than the acyl chain length. The molecular-level reasons for such asymmetric interactions cannot be deciphered from the results presented here, but they are likely to involve orientational effects caused by favorable hydrogen bonding between ceramide and POPC. This is likely for at least two reasons. First, the long-chain base has two hydrogen-bond donating and accepting functional groups (1-OH and 3-OH), whereas the *N*-linked acyl chain has a hydrogen-bond accepting group (carbonyl ester oxygen) and the NH, which can donate hydrogen for intermolecular interactions. Second, if the hydrophobic interactions among matching saturated chains were the most dominant forces in stabilizing the intermolecular interactions, one would not expect the asymmetric ceramide analogs to have behaved differently (Figs. 4 and 5), since both analogs contained an equal number of carbons in their two chains and were fully saturated (except for the *trans* double bond in the long-chain base).

It is known that when acyl chain lengths are varied in saturated PC bilayers, the length of the *sn*-2 acyl chain is more effective at increasing the T_m than an equal acyl chain in the *sn*-1 position. For example, 14:0/18:0-PC has a gel-liquid crystalline phase transition temperature of 38°C, whereas 18:0/14:0-PC has a T_m of 30°C (43). This

difference in T_m may relate to effects of the large phosphocholine headgroup on the most efficient acyl chain packing in the hydrophobic core of the bilayer. For ceramides, which lack a large headgroup, the nonequal effects of hydrocarbon chain lengths must derive from factors other than headgroup-influenced lateral interactions.

Further support for the inequality of the long-chain base and the *N*-linked acyl chain came from our ^{2}H NMR analysis of site-deuterated stearoyl-ceramide analogs (Fig. 5): one with two deuterons at position C12 in the long-chain base, and the other with two deuterons at C10 in the acyl chain. In stearoyl SM, the deuterons from these two positions showed much closer quadrupolar splitting values (Fig. S6) (30), suggesting that they had similar mobilities. In the deuterated ceramide analogs dissolved in POPC, the deuterons on the long-chain base showed less mobility than the deuterons on the acyl chain at temperatures between 20°C and 35°C. This would support the notion that stronger or preferential interactions between the long-chain base and the palmitoyl residue of POPC led to a more restricted mobility of C12 in the long-chain base compared with C10 in the *N*-linked acyl chain. This may relate to the umbrella effect of the POPC large headgroup (39), since the bulkier long-chain base chain interacts more easily with a less bulky palmitoyl chain of POPC and vice versa. The lower mobility of the long-chain base chain implies that this chain melts (or becomes mobile) at a slightly higher temperature than does the acyl chain in the lipid mixtures used here.

Ceramides with unequal lengths of the long-chain base and *N*-linked acyl chains can be considered to display a chain-length mismatch between the two chains (44), and an extensive chain-length mismatch would be expected to disorder the terminal part of the longer chain. It has been suggested that such a mismatch among SMs can explain why the gel-phase stability in fully hydrated SM bilayers does not increase significantly with acyl chain lengths above C18:0 (44). The gel-phase stability of fully hydrated ceramide crystals is also dependent, to some extent, on the acyl chain length (12) (Table S1), but much more so on the length of the long-chain base (Table S1).

CONCLUSION

We have shown that ceramide-colipid interactions are influenced more by the length of the long-chain base than the length of the *N*-linked acyl chains. This finding implies that ceramide-colipid interactions are asymmetric. This conclusion is further supported by results obtained with asymmetric ceramide analogs (d20:1/13:0 or d16:1/17:0), since the analog with a longer sphingoid base showed a higher gel-phase thermostability and had a higher chain order (quadrupole splitting) in the sphingoid base than in the acyl chain at comparable deuteron positions and temperatures. We argue that the asymmetric location of functional groups involved in hydrogen bonding may explain the asymmetric nature of ceramide-colipid interactions. Asymmetric interactions among ceramides are likely to affect the propensity of ceramides to form ceramide-rich platforms, which have been suggested to be important for the initiation of apoptosis (8). However, since mammalian ceramides more often have variable acyl chain lengths than variable long-chain base lengths, this may suggest that variable acyl chain lengths give unique properties to ceramides that do not necessarily influence gel-phase properties dramatically. These unique properties of ceramides could be important for their specific interactions with membrane proteins, and for their substrate properties in the biosynthesis of more complex sphingolipids.

SUPPORTING MATERIAL

Supporting Materials and Methods, one scheme, six figures, and one table are available at http://www.biophysj.org/biophysj/supplemental/S0006-3495(17)30111-X.

AUTHOR CONTRIBUTIONS

M.A.A.S. and T.Y. performed experiments. T.Y. contributed important reagents. All authors contributed to the interpretation of data and to the writing of the manuscript. All authors approved the final version of the manuscript.

ACKNOWLEDGMENTS

We thank Dr. Thomas Nyholm for helpful discussions during the writing of the manuscript.

This work was supported by grants from the Academy of Finland, the Sigrid Juselius Foundation, the Jane and Aatos Erkko Foundation, the Ella and Georg Ehrnrooth Foundation, and the Magnus Ehrnrooth Foundation (to J.P.S.). M.M. received support from the ERATO Lipid Active Structure Project of the Japan Science and Technology Agency and Grant-In-Aids for Scientific Research (A) (No. 25242073) from MEXT, Japan. T.Y. was partly supported by the International Joint Research Promotion Program at Osaka University.

REFERENCES

1. Merrill, A. H., Jr., E. M. Schmelz, …, E. Wang. 1997. Sphingolipids—the enigmatic lipid class: biochemistry, physiology, and pathophysiology. *Toxicol. Appl. Pharmacol.* 142:208–225.
2. Merrill, A. H., Jr. 2002. De novo sphingolipid biosynthesis: a necessary, but dangerous, pathway. *J. Biol. Chem.* 277:25843–25846.
3. Merrill, A. H., Jr., and K. Sandhoff. 2002. Sphingolipids: metabolism and cell signaling. *In* Biochemistry of Lipids, Lipoproteins and Membranes, 4th ed. D. E. Vance and J. E. Vance, editors. Elsevier, Oxford, UK, pp. 373–407.
4. Bouwstra, J. A., F. E. Dubbelaar, …, M. Ponec. 1999. The role of ceramide composition in the lipid organisation of the skin barrier. *Biochim. Biophys. Acta.* 1419:127–136.
5. Bouwstra, J. A., P. L. Honeywell-Nguyen, …, M. Ponec. 2003. Structure of the skin barrier and its modulation by vesicular formulations. *Prog. Lipid Res.* 42:1–36.
6. Kolesnick, R., and Y. A. Hannun. 1999. Ceramide and apoptosis. *Trends Biochem. Sci.* 24:224–225, author reply 227.

7. Barenholz, Y., and T. E. Thompson. 1980. Sphingomyelins in bilayers and biological membranes. *Biochim. Biophys. Acta.* 604:129–158.
8. Slotte, J. P. 2013. Biological functions of sphingomyelins. *Prog. Lipid Res.* 52:424–437.
9. Maula, T., Y. J. E. Isaksson, …, J. P. Slotte. 2013. 2NH and 3OH are crucial strctural requirements in sphingomyelin for sticholysin II binding and pore formation in bilayer membranes. *Biochim. Biophys. Acta.* 1828:1390–1395.
10. Maula, T., B. Urzelai, and J. Peter Slotte. 2011. The effects of N-acyl chain methylations on ceramide molecular properties in bilayer membranes. *Eur. Biophys. J.* 40:857–863.
11. Maula, T., I. Artetxe, …, J. P. Slotte. 2012. Importance of the sphingoid base length for the membrane properties of ceramides. *Biophys. J.* 103:1870–1879.
12. Maula, T., M. A. Al Sazzad, and J. P. Slotte. 2015. Influence of hydroxylation, chain length, and chain unsaturation on bilayer properties of ceramides. *Biophys. J.* 109:1639–1651.
13. Nybond, S., Y. J. Bjorkqvist, …, J. P. Slotte. 2005. Acyl chain length affects ceramide action on sterol/sphingomyelin-rich domains. *Biochim. Biophys. Acta.* 1718:61–66.
14. Sot, J., F. J. Aranda, …, A. Alonso. 2005. Different effects of long- and short-chain ceramides on the gel-fluid and lamellar-hexagonal transitions of phospholipids: a calorimetric, NMR, and x-ray diffraction study. *Biophys. J.* 88:3368–3380.
15. Chiantia, S., N. Kahya, and P. Schwille. 2007. Raft domain reorganization driven by short- and long-chain ceramide: a combined AFM and FCS study. *Langmuir.* 23:7659–7665.
16. Pinto, S. N., L. C. Silva, …, M. Prieto. 2011. Effect of ceramide structure on membrane biophysical properties: the role of acyl chain length and unsaturation. *Biochim. Biophys. Acta.* 1808:2753–2760.
17. Maula, T., M. Kurita, …, J. P. Slotte. 2011. Effects of sphingosine 2N- and 3O-methylation on palmitoyl ceramide properties in bilayer membranes. *Biophys. J.* 101:2948–2956.
18. Skolová, B., B. Janůšová, …, K. Vávrová. 2013. Ceramides in the skin lipid membranes: length matters. *Langmuir.* 29:15624–15633.
19. Megha, and E. London. 2004. Ceramide selectively displaces cholesterol from ordered lipid domains (rafts): implications for lipid raft structure and function. *J. Biol. Chem.* 279:9997–10004.
20. Alanko, S. M., K. K. Halling, …, B. Ramstedt. 2005. Displacement of sterols from sterol/sphingomyelin domains in fluid bilayer membranes by competing molecules. *Biochim. Biophys. Acta.* 1715:111–121.
21. Castro, B. M., L. C. Silva, …, M. Prieto. 2009. Cholesterol-rich fluid membranes solubilize ceramide domains: implications for the structure and dynamics of mammalian intracellular and plasma membranes. *J. Biol. Chem.* 284:22978–22987.
22. Busto, J. V., J. Sot, …, A. Alonso. 2010. Cholesterol displaces palmitoylceramide from its tight packing with palmitoylsphingomyelin in the absence of a liquid-disordered phase. *Biophys. J.* 99:1119–1128.
23. Ekman, P., T. Maula, …, J. P. Slotte. 2015. Formation of an ordered phase by ceramides and diacylglycerols in a fluid phosphatidylcholine bilayer—correlation with structure and hydrogen bonding capacity. *Biochim. Biophys. Acta.* 1848:2111–2117.
24. Al Sazzad, M. A., and J. P. Slotte. 2016. Effect of phosphatidylcholine unsaturation on the lateral segregation of palmitoyl ceramide and palmitoyl dihydroceramide in bilayer membranes. *Langmuir.* 32:5973–5980.
25. Dutagaci, B., J. Becker-Baldus, …, C. Glaubitz. 2014. Ceramide-lipid interactions studied by MD simulations and solid-state NMR. *Biochim. Biophys. Acta.* 1838:2511–2519.
26. Sklar, L. A., B. S. Hudson, and R. D. Simoni. 1977. Conjugated polyene fatty acids as fluorescent probes: synthetic phospholipid membrane studies. *Biochemistry.* 16:819–828.
27. Cohen, R., Y. Barenholz, …, A. Dagan. 1984. Preparation and characterization of well defined D-erythro sphingomyelins. *Chem. Phys. Lipids.* 35:371–384.
28. Kuklev, D. V., and W. L. Smith. 2004. Synthesis of four isomers of parinaric acid. *Chem. Phys. Lipids.* 131:215–222.
29. Lakowicz, J. R. 1999. Principles of Fluorescence Spectroscopy. Kluwer Academic/Plenum Publishers, New York.
30. Matsumori, N., T. Yasuda, …, M. Murata. 2012. Comprehensive molecular motion capture for sphingomyelin by site-specific deuterium labeling. *Biochemistry.* 51:8363–8370.
31. Silva, L. C., R. F. de Almeida, …, M. Prieto. 2007. Ceramide-domain formation and collapse in lipid rafts: membrane reorganization by an apoptotic lipid. *Biophys. J.* 92:502–516.
32. Sklar, L. A., G. P. Miljanich, and E. A. Dratz. 1979. Phospholipid lateral phase separation and the partition of *cis*-parinaric acid and *trans*-parinaric acid among aqueous, solid lipid, and fluid lipid phases. *Biochemistry.* 18:1707–1716.
33. Castro, B. M., R. F. de Almeida, …, M. Prieto. 2007. Formation of ceramide/sphingomyelin gel domains in the presence of an unsaturated phospholipid: a quantitative multiprobe approach. *Biophys. J.* 93:1639–1650.
34. Silva, L., R. F. de Almeida, …, M. Prieto. 2006. Ceramide-platform formation and -induced biophysical changes in a fluid phospholipid membrane. *Mol. Membr. Biol.* 23:137–148.
35. Sot, J., M. Ibarguren, …, A. Alonso. 2008. Cholesterol displacement by ceramide in sphingomyelin-containing liquid-ordered domains, and generation of gel regions in giant lipidic vesicles. *FEBS Lett.* 582:3230–3236.
36. Veiga, M. P., J. L. Arrondo, …, A. Alonso. 1999. Ceramides in phospholipid membranes: effects on bilayer stability and transition to nonlamellar phases. *Biophys. J.* 76:342–350.
37. Carrer, D. C., and B. Maggio. 1999. Phase behavior and molecular interactions in mixtures of ceramide with dipalmitoylphosphatidylcholine. *J. Lipid Res.* 40:1978–1989.
38. Ali, M. R., K. H. Cheng, and J. Huang. 2006. Ceramide drives cholesterol out of the ordered lipid bilayer phase into the crystal phase in 1-palmitoyl-2-oleoyl-sn-glycero-3-phosphocholine/cholesterol/ceramide ternary mixtures. *Biochemistry.* 45:12629–12638.
39. Huang, J., J. T. Buboltz, and G. W. Feigenson. 1999. Maximum solubility of cholesterol in phosphatidylcholine and phosphatidylethanolamine bilayers. *Biochim. Biophys. Acta.* 1417:89–100.
40. Huang, J., and G. W. Feigenson. 1999. A microscopic interaction model of maximum solubility of cholesterol in lipid bilayers. *Biophys. J.* 76:2142–2157.
41. Mabrey, S., and J. M. Sturtevant. 1976. Investigation of phase transitions of lipids and lipid mixtures by sensitivity differential scanning calorimetry. *Proc. Natl. Acad. Sci. USA.* 73:3862–3866.
42. Heberle, F. A., M. Doktorova, …, G. W. Feigenson. 2013. Hybrid and nonhybrid lipids exert common effects on membrane raft size and morphology. *J. Am. Chem. Soc.* 135:14932–14935.
43. Koynova, R., and M. Caffrey. 1998. Phases and phase transitions of the phosphatidylcholines. *Biochim. Biophys. Acta.* 1376:91–145.
44. Kodama, M., and Y. Kawasaki. 2010. Structural role of mismatched C-C bonds in a series of d-erythro-sphingomyelins as studied by DSC and electron microscopy. *Chem. Phys. Lipids.* 163:514–523.

Biophysical Journal, Volume *112*

Supplemental Information

The Long-Chain Sphingoid Base of Ceramides Determines Their Propensity for Lateral Segregation

Md. Abdullah Al Sazzad, Tomokazu Yasuda, Michio Murata, and J. Peter Slotte

Synthesis of d19:1/16:0 ceramide

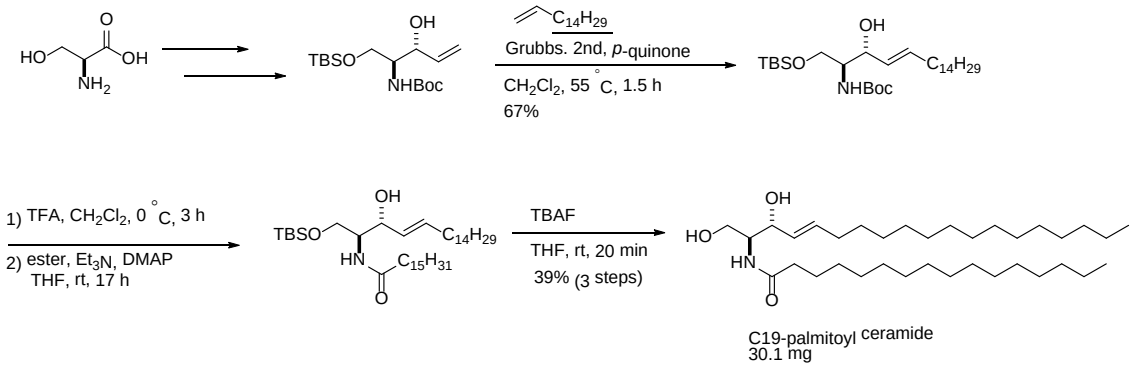

To a solution of olefin **2** in CH_2Cl_2 was added 1-hexadecene and Grubbs catalyst 2nd generation at room temperature. After the reaction mixture was stirred for 2h under reflux, solvent was removed in vacuo to give crude products. Column chromatography on silica gel gave **3** as a colorless oil.

1-hexadecene was synthesized from 1-pentadecanol by oxidation and Wittig reaction.

To a solution of **3** in CH_2Cl_2 was added trifluoroacetic acid at 0°C. After the reaction mixture was stirred for 3 h at 0°C, the reaction was quenched with Et3N, and the resulting mixture was evaporated to give the crude amine, which was subjected to the next reaction without further purification. To a solution of the crude amine in THF were added DMAP, and *p*-nitrophenyl hexadecanoate. After the reaction mixture was stirred for 17 h at room temperature, the mixture was evaporated. Purification by silica gel column chromatography afforded TBS-protected ceramide as a white solid. To a solution of the protected ceramide in THF was added TBAF at 0°C. After the reaction mixture was stirred for 20 min at room temperature, H_2O was added to the solution and the solvent was evaporated. Purification by silica gel column chromatography afforded C19-palmitoyl ceramide as a white solid. Molecular identity was verified by mass spectrometry (LQT-Orbitrap XL) and NMR (Jeol ECS 400).

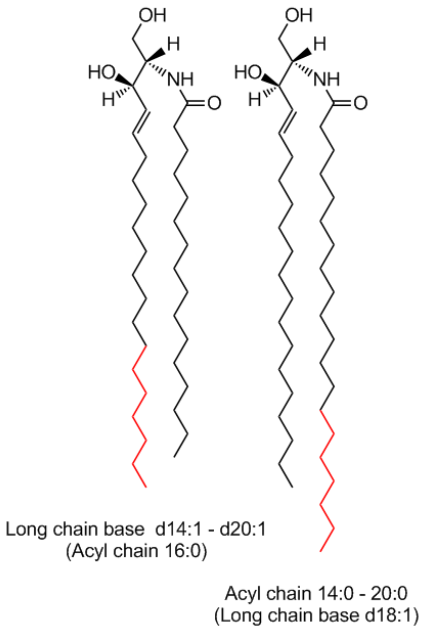

SCHEME S1. Long-chain base and acyl chain length ceramide analog used in the study. The long-chain base length varied between 14 and 20 carbons (with 16:0 as *N*-linked acyl chain), and the *N*-linked acyl chain varied between 14 and 20 carbons (with d18:1 as long-chain base).

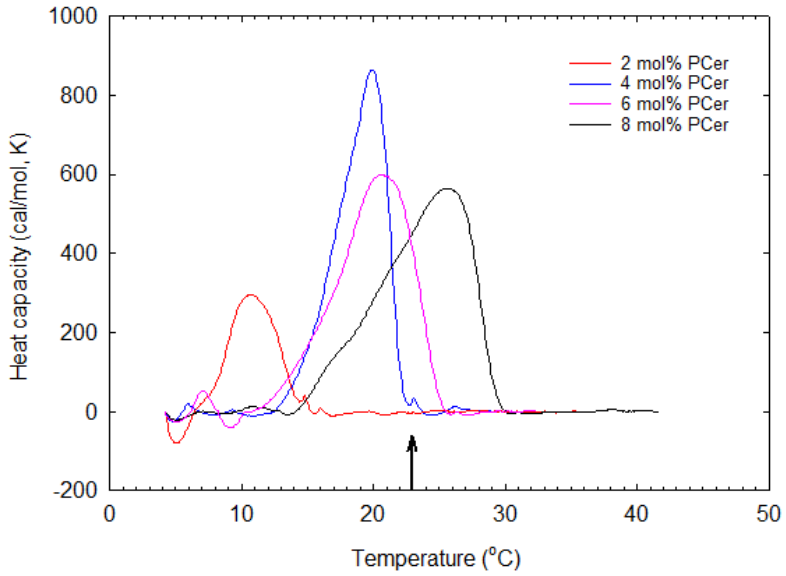

FIGURE S1. DSC analysis of ceramide gel phase melting as a function of ceramide concentration. The heating scan rate was 1 °C/min, and only upscan data are shown. The arrow indicate 23 °C, the temperature of tPA fluorescence lifetime analysis in Fig 1, allowing for easy comparison of DSC data with tPA fluorescence lifetime data.

TABLE S1. Main transition temperature (T_m) of some hydrated ceramide analogs. T_m values given are for heating scans (1 °C /min).

Ceramide	T_m (°C)
d18:1/12:0	85.7[a]
d18:1/16:0	91.5[a]
d18:1/18:0	91.1[a]
d18:1/20:0	92.6
d15:1/16:0	82.4
d16:1/16:0	84.8
d17:1/16:0	87.8
d18:1/16:0	91.5
d20:1/16:0	96.4

Values marked [a] are taken from (12)

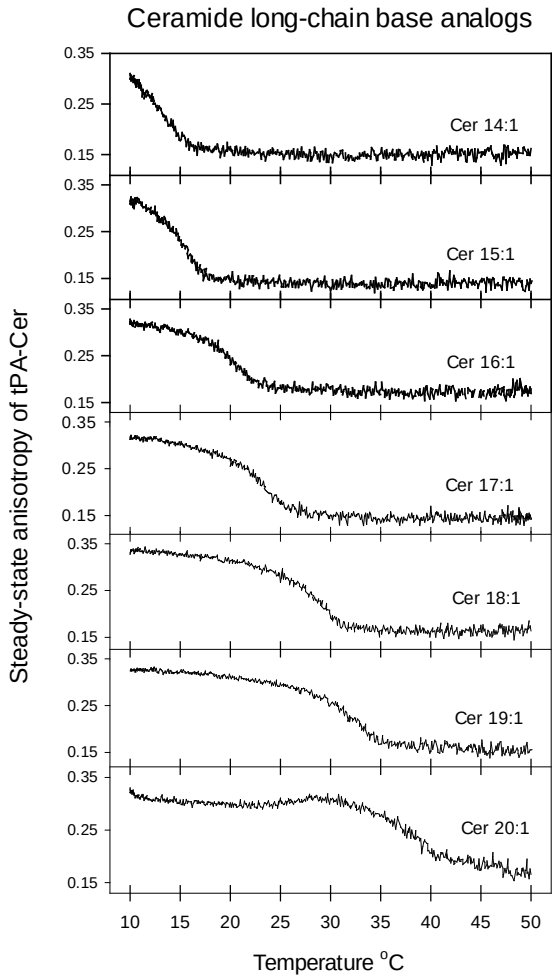

FIGURE S2. tPA-Cer anisotropy in bilayers containing ceramide long-chain base sanalogs. The temperature scan rate was 5 °C/min, and curves are representative of 2-3 replicates.

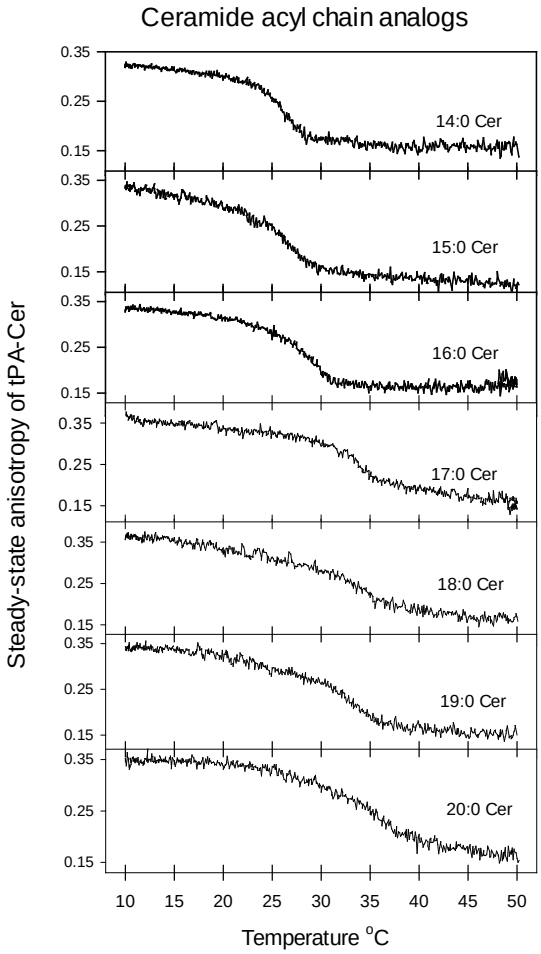

FIGURE S3. tPA-Cer anisotropy in bilayers containing ceramide acyl-chain analogs. The temperature scan rate was 5 °C/min, and curves are representative of 2-3 replicates.

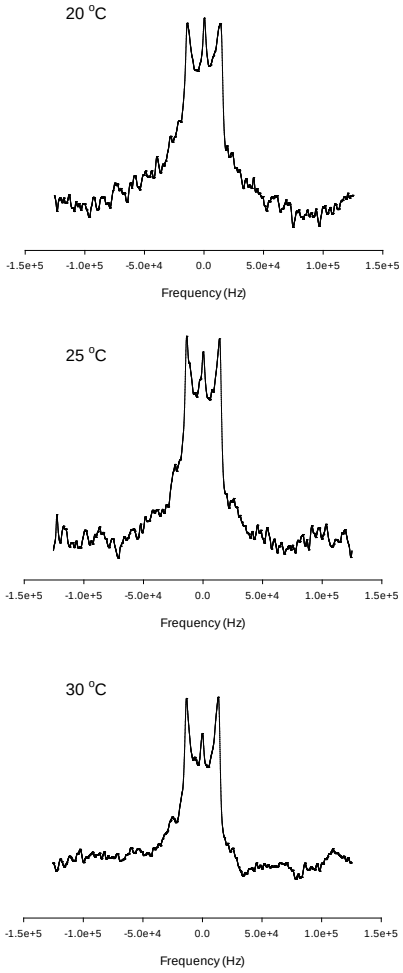

FIGURE S4. ^{2}H NMR spectra of long-chain base deuterated (d2) stearoyl ceramide. The composition was 10 mol% stearoyl ceramide in POPC, and the temperature 20, 25 and 30 °C. The ceramide was deuterated (d2) at the 10 position of the long-chain base.

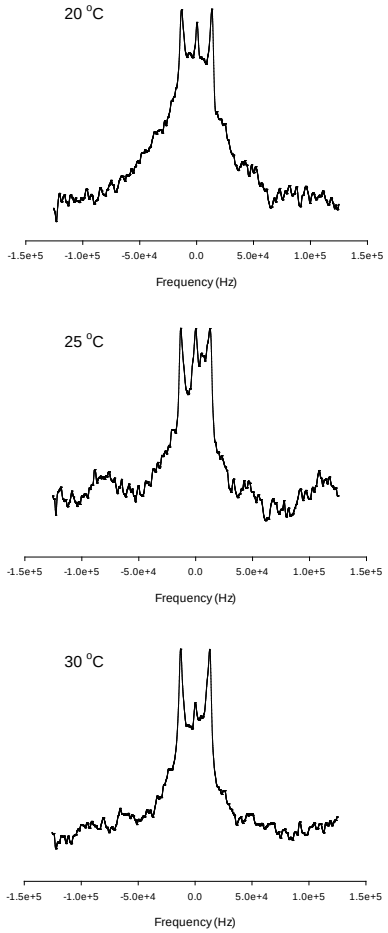

FIGURE S5. ^{2}H NMR spectra of acyl chain deuterated (d2) stearoyl ceramide. The composition was 10 mol% stearoyl ceramide in POPC, and the temperature 20, 25 and 30 °C. The ceramide was deuterated (d2) at the 12 position of the acyl chain.

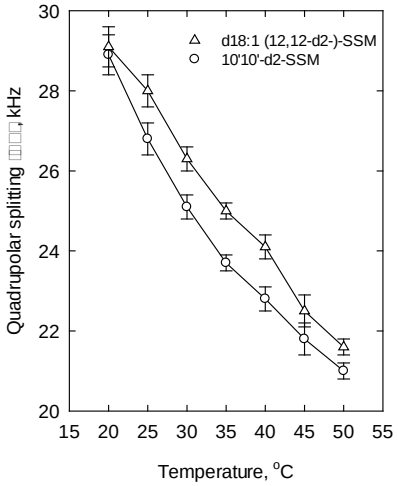

FIGURE S6. Quadrupolar splitting of site-deuterated long-chain base or acyl chain in stearoyl sphingomyelin (SSM, 10 mol%) in POPC (90 mol%) bilayers. The sphingosine long-chain base was site-deuterated (d2) at carbon 10, or the stearoyl acyl chain at carbon 12. The $\Delta\nu$ was determined as a function of temperature for the two SSM analogs.

Supplemental reference

12. Maula, T., M. A. Al Sazzad, and J. P. Slotte. 2015. Influence of Hydroxylation, Chain Length, and Chain Unsaturation on Bilayer Properties of Ceramides. Biophys J 109: 1639-1651.